Phase Transitions of Scaling Functions Derived from Experimental Time Series

R. Stoop and J. Parisi

Physics Institute, University of Zurich, CH-8001 Zurich, Switzerland

Z. Naturforsch. **47a**, 819–825 (1992); received April 21, 1992

The occurrence of phase transitions in dynamical systems is intimately related to the analyticity properties of the thermodynamical functions. Such effects are believed to be of generic nature (for example, homoclinic tangency points). For one-dimensional maps, their existence has been proven for both the probabilistic and the dynamical scaling functions (that is, the $f(\alpha)$ and $\Phi(\lambda)$ spectra, respectively). With the help of simple model systems, we elucidate the different combinations in which the two types of phase transitions (namely, in the $f(\alpha)$ and $\Phi(\lambda)$ spectra) can appear. Moreover, we demonstrate the numerical evidence of phase-transition-like behavior in both spectra derived from experimental time series of laser and semiconductor systems. Finally, we discuss new aspects for the evaluation of the thermodynamic functions from time series.

1. Introduction

In the last years, the characterization of experimental dynamical systems through their scaling behavior has become a wide field of research, since it was realized that for a description of these systems various mutually independent quantities can be useful. The most prominent among these characterizations are the fractal dimensions and the Lyapunov exponents, on one hand, and different concepts of entropy and the complexity, on the other hand. For a more refined description of a system, also fluctuations of at least the first two quantities should be taken into account. This can be achieved by the evaluation of scaling functions of fractal dimensions and Lyapunov exponents.

In this contribution, we are mainly concerned with the characterization of the dynamical scaling behavior, i.e., the characterization of a system with the help of its Lyapunov exponents and their scaling functions. We show that in the dynamical scaling functions of experimental germanium semiconductor and ruby NMR-laser data different phase-transition-like behavior can be observed, which indicates the usefulness of the thermodynamic approach to dynamical systems. A mathematical description of an appropriate dynamical system starts with the definition of a suitable generating partition. For a given system, many diverse generating partitions are possible, depending on the point of view one is interested in. For example, if statistical behavior in the phase space is considered ("fractal dimension" or "probabilistic" approach), a fixed size partition can be used. If, however, one would like to obtain information about the dynamical behavior, a partition is necessary which is "compatible" with the dynamical scaling behavior, i.e., a dynamical partition is requested.

Reprint requests to Priv.-Doz. Dr. Jürgen Parisi, Physics Institute, University of Zurich, Schönberggasse 9, CH-8001 Zurich, Switzerland.

2. The Partition Function

Given a dynamical partition of M symbols, we proceed in analogy to statistical mechanics and define the partition function for an attractor or repeller A [1]:

$$GZ(q,\beta,n) = \sum_{j\in(1,\ldots,M)^n} l_i^{\beta}\, p_j^{q}. \tag{1}$$

Here, the size of the j'th region R_j of the partition is denoted by l_j, whereas the probability to fall into this region is labeled by p_j ($p_j = \int_{R_j} \varrho(x)\,\mathrm{d}x$, where $\varrho(x)$ means the natural measure). n gives the "level" of the partition. To account for the nonisotropy of the attractor, l, p, β, q can be thought of as vectors, β and q are sometimes called "filtering exponents". Local scaling of l and p in n is expected; in this way, the scaling exponents ε and α are defined through

$$l_j = e^{-n\varepsilon_j}, \tag{2}$$

and

$$p_j = l_j^{\alpha_j}. \tag{3}$$

Again, these exponents should be considered as vectors. Using these scaling exponents, a "generalized free

0932-0784 / 92 / 0700-0819 $ 01.30/0. – Please order a reprint rather than making your own copy

energy" GF can be derived from the partition function [2]:

$$GF(q,\beta) = \lim_{n\to\infty} \frac{1}{n} \log \sum_{j\in(1,\ldots,M)^n} e^{-n\varepsilon_j(\alpha_j q+\beta)}. \quad (4)$$

A generalized "entropy function" $GS(\alpha,\varepsilon)$ is then introduced through the "global"scaling assumption that the number of regions N which have scaling exponents between (α,ε) and $(\alpha+d\alpha,\varepsilon+d\varepsilon)$ scales as

$$N(\alpha,\varepsilon)\,d\alpha\,d\varepsilon \sim e^{GS(\alpha,\varepsilon)}\,d\alpha\,d\varepsilon. \quad (5)$$

Writing the partition function formally as an integral, via a saddle-point approach the relationship between the generalized free energy GF and the generalized entropy GS is found [2]:

$$GS(\alpha,\varepsilon) = GF(q,\beta) + (\langle\alpha\rangle q + \beta)\langle\varepsilon\rangle, \quad (6)$$

where the brackets indicate that those values of α and ε which lead to the maximum of GZ (as a function of given q and β) have been chosen. In the following, we will omit the brackets. The generalized free energy GF or the generalized entropy GS describe in this way equivalently the scaling behavior of the dynamical system. Note that the information-theoretical "Renyi entropies" evolve from (4) for $\beta = 0$. By restriction to $q = 0$, the associated entropy to be considered later on is denoted by $GS(\varepsilon)$. For similar approaches related to the dynamical behavior, see [3]. We point out that also the fractal dimensions and the corresponding entropy-like function $f(\alpha)$ can be obtained from $GF(q,\beta)$ [1, 4, 5, 6].

3. Model Systems

The simplest scaling behavior is provided by the well-known asymptotic tent map. This system leads to a strictly convex function $GS(\varepsilon)$. Moreover, the function $f(\alpha)$ can be recovered by $GS(\varepsilon)$. To account for more general situations, it has been proposed to include probabilities p_j as in (1) which cannot be expressed through the derivative of the dynamical map. For the example of a three-scale Cantor set, we find the scaling behavior shown in Figure 1. A general dynamical system might be only asymptotically self-similar, nonhyperbolic, or without a complete symbolic tree. Here, the situation must be expected to be even more complicated [7, 8].

A careful investigation of the free energy function in the nonhyperbolic case shows that, due to singularities in the natural measure, the free energy is no longer real-analytic. Such behavior can be interpreted as a phase transition. For one-dimensional maps, the action of the dynamical partition can be described with the help of the generalized Frobenius-Perron operator [9]; for some of these maps, the natural measure then evolves as the eigenfunction of this operator for "temperature" $\beta = 1$. It can, furthermore, be seen that (in analogy to most "real" phase transitions) different eigenfunctions belong to different phases which can be characterized by different values of the temperature β [10]. In this way, they indicate the different symmetry or order properties of the different phases. For the dynamical and the probabilistic approach, phase-transition-like behavior has been detected in a number of prominent model cases, such as the Hénon map, the circle map, and the logistic map [6, 10], as well as the Lorenz system [11]. By considering again Fig. 1, one even suspects that different kinds of combinations of phase transitions in the $f(\alpha)$ and $GS(\varepsilon)$ spectra are possible, depending on the place within the support of $GS(\alpha,\varepsilon)$ where this effect is located [8].

4. Application to Experimental Data

From the outline, it can be expected that phase-transition-like behavior could also be observed in experimental systems. For experimental data, it has been proposed in [6] to use directly the symbolic dynamics approach and to consider strings of symbols obtained from an experiment. This approach, however, is not as easy to follow as it seems, although interesting progress has been obtained for the Henon and the Lozi maps in [12]: there is no general recipe of how to obtain a generating partition even for model systems [13]. In the following, we therefore use a different formalism adapted to the generic situation of random sampling. We assume for the probabilistic approach that no distribution of length scales ε is needed; for the dynamical approach, it is customary to sample in time. Instead of the scaling exponent ε and the corresponding spectrum $GS(\varepsilon)$, we focus on the Lyapunov exponent λ and the scaling function of Lyapunov exponents, $\phi(\lambda)$. As a consequence, (4) changes to the following set of well-known relations that emanate from (1).

For the probabilistic approach,

$$\tau(q) = \lim_{\epsilon\to 0} \frac{\log\langle P(B(x,\epsilon))^{q-1}\rangle}{\log\epsilon}, \quad (7)$$

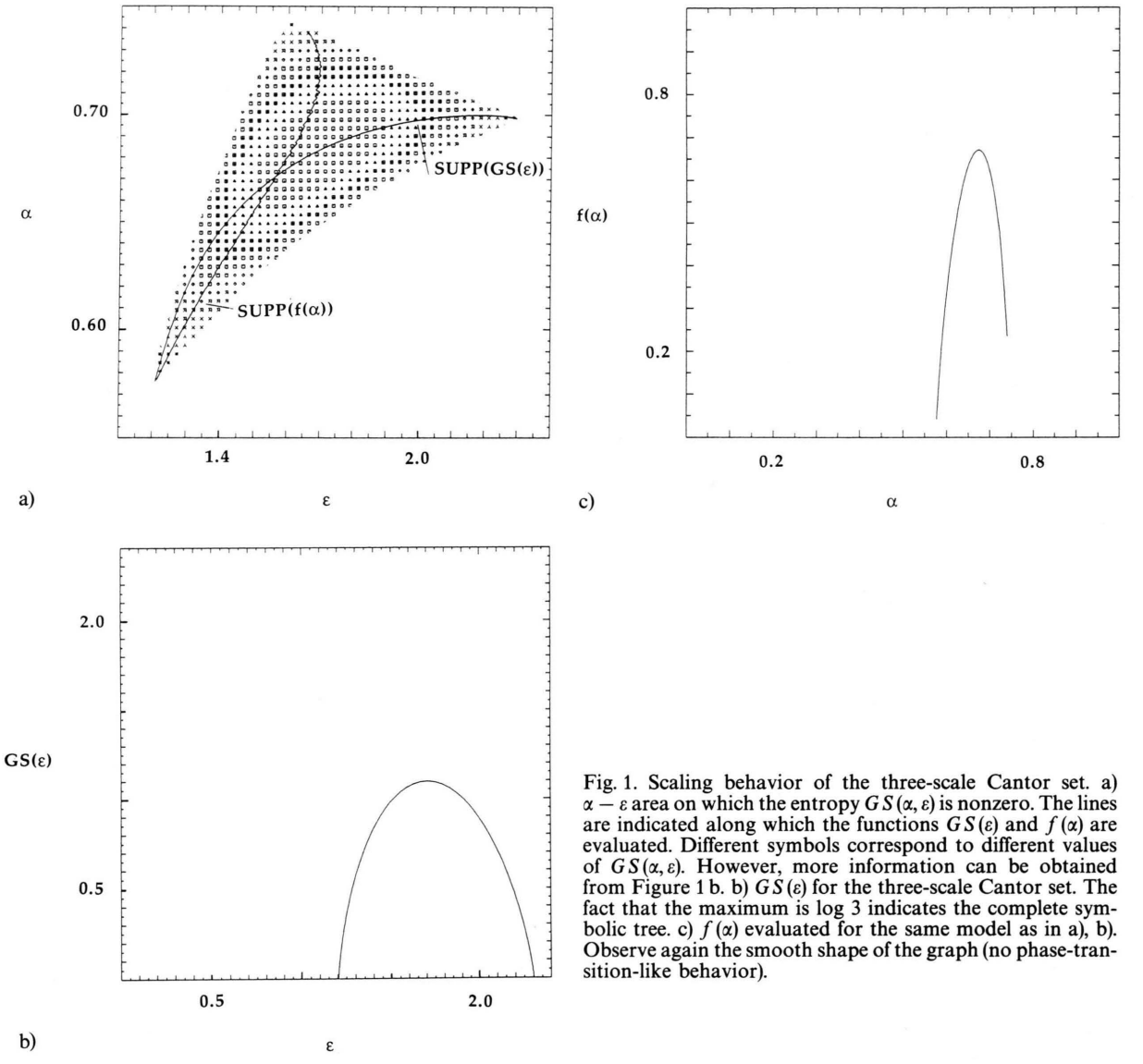

Fig. 1. Scaling behavior of the three-scale Cantor set. a) $\alpha - \varepsilon$ area on which the entropy $GS(\alpha, \varepsilon)$ is nonzero. The lines are indicated along which the functions $GS(\varepsilon)$ and $f(\alpha)$ are evaluated. Different symbols correspond to different values of $GS(\alpha, \varepsilon)$. However, more information can be obtained from Figure 1 b. b) $GS(\varepsilon)$ for the three-scale Cantor set. The fact that the maximum is log 3 indicates the complete symbolic tree. c) $f(\alpha)$ evaluated for the same model as in a), b). Observe again the smooth shape of the graph (no phase-transition-like behavior).

$$P(B(x, \epsilon)) \sim \epsilon^{\alpha(x)} \tag{8}$$

replaces the expression for the free energy {where $P(B(x, \epsilon)\}$ is the probability for a randomly chosen point of having a smaller distance than ϵ from point x). The entropy-like quantity $f(\alpha)$ is then found as

$$f(\alpha) = \alpha q - \tau(q), \tag{9}$$

where

$$\alpha(q) = \frac{\mathrm{d}\tau(q)}{\mathrm{d}q} \tag{10}$$

and

$$P(\alpha, \epsilon)\,\mathrm{d}\alpha \sim \epsilon^{\alpha - f(\alpha)}\,\mathrm{d}\alpha\,. \tag{11}$$

For the dynamical approach,

$$\Lambda(\beta) = \lim_{n \to \infty} \frac{\log \langle (DF\, a^{n,+})^{-(\beta-1)} \rangle}{\log T} \tag{12}$$

replaces the expression of the free energy (where $T := e^{-n}$, and $DF\, a^{n,+}$ denotes the product of the stretching factors of absolute values larger than one in the tangent bundle associated with the n-times iter-

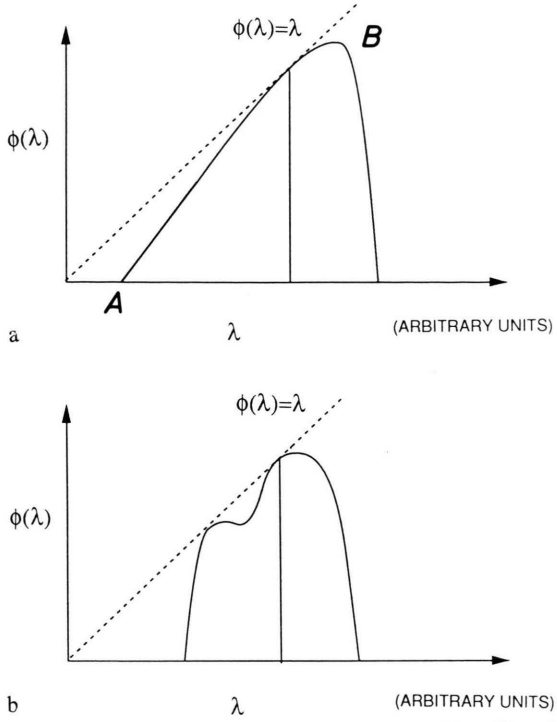

Fig. 2. a) Schematic drawing of a phase-transition-like effect caused by the coexistence of a repelling fixed point A and an attractor B for the dynamical function $\phi(\lambda)$. b) Schematic drawing of the scaling function $\phi(\lambda)$ in presence of a crisis.

ated dynamical map Fa, and

$$P(x, T) \sim T^{1/n \log(DF a^{n,+}(x))}. \tag{13}$$

In this case, the entropy-like quantity $\phi(\lambda)$ is obtained as

$$\phi(\lambda) = \beta\lambda - \Lambda(\beta), \tag{14}$$

where

$$\lambda(\beta) = \frac{\mathrm{d}\Lambda(\beta)}{\mathrm{d}\beta} \tag{15}$$

and

$$P(\lambda, k)\,\mathrm{d}\lambda \sim e^{-k(-\phi(\lambda)+\lambda)}\,\mathrm{d}\lambda. \tag{16}$$

Note again that, in a strict sense, the interpretation of $P(x, T)$ as a probability holds only for the hyperbolic case.

For each of the two approaches, a thermodynamic formalism [14] can be formulated separately. The case of the generalized partition function has been identified with an isobar-isotherm ensemble [15]. The simplest example of a phase-transition-like behavior in both the probabilistic and the present dynamical approach is provided by the coexistence of a repeller and an attractor. It has been pointed out earlier that phase-transition-like effects are to be expected generically from the existence of homoclinic tangency points [8, 16, 17]. Qualitatively different effects are obtained from systems at a crisis [18, 19] or from the presence of a marginally unstable fixed point, as described in [11]. In Fig. 2, a schematic picture of the two cases is shown.

5. Experimental Evidence

In this section, results from two experiments are discussed. For experimental systems, the information about the dynamical system is provided by the help of a time series. By use of an embedding process, the attractor is reconstructed and the generalized dimensions, the generalized Lyapunov exponents, and the corresponding scaling functions can be calculated. Different concept variants for the calculation of Lyapunov exponents from time series [20, 21] were used, which yielded identical results. In Fig. 3, we show the dynamical scaling function $\phi(\lambda)$ for Hénon's map from an embedded time series. Observe the straight-line behavior on the l.h.s. of the scaling function. This phase-transition-like effect is due to the presence of homoclinic tangency points. We emphasize that this straight-line behavior can be demonstrated to occur also when using the generalized formalism (discussed in Sect. 2) for nonhyperbolic model systems (work in preparation). As one expects, phase-transition-like phenomena are detectable as well in experimental data.

For the experiments, the numerical procedure started from data files of minimal 100,000 integers with a 12 bit resolution, rescaled to integers in the range from 0 to 10,000. To perform the numerical treatment advocated in the last section, it would be desirable to have full knowledge about the grammar of the experimental system. If this is not the case, it cannot be guaranteed that the rescaling with the number n of time steps (see, e.g., (13)) provides stable results for the scaling function. For experimental applications, it must, therefore, be checked that varying n in a considerable interval does not change the form of the scaling function, with exception of the marginal tails. In the experiments reported below, such situations have been selected.

As the first example, we consider a p-germanium semiconductor system [22]. Its nonlinear dynamics

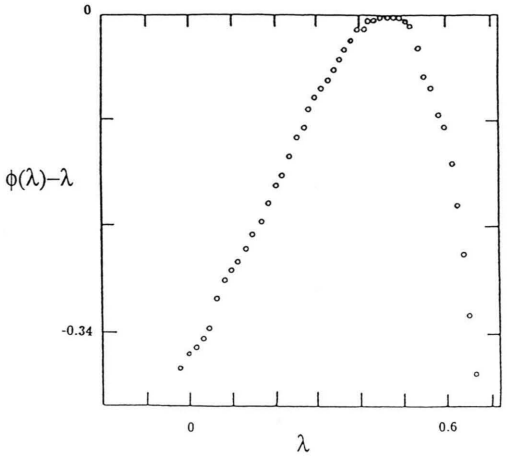

Fig. 3. Dynamical scaling function $\phi(\lambda)$ for Hénon's map from an embedded time series. The phase-transition-like effect is due to the presence of homoclinic tangency points.

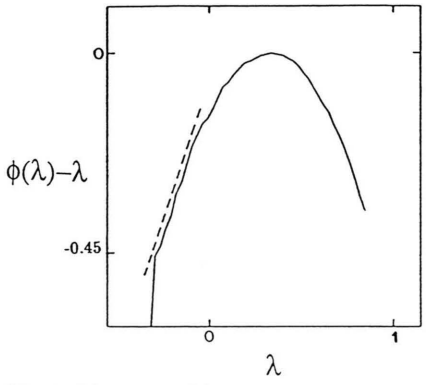

Fig. 4. Phase-transition-like effect in the dynamical scaling function $\phi(\lambda)$ for the experimental p-Ge semiconductor sample.

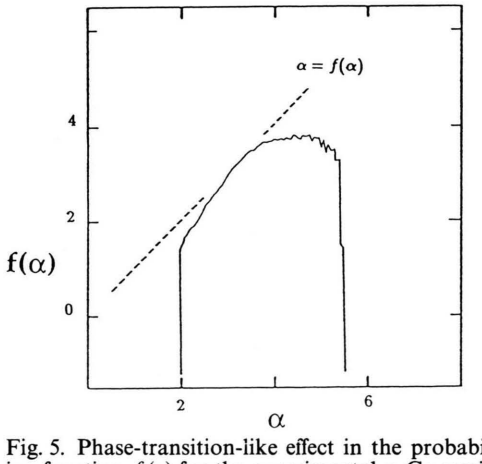

Fig. 5. Phase-transition-like effect in the probabilistic scaling function $f(\alpha)$ for the experimental p-Ge semiconductor sample.

consisting of spontaneous current oscillations results from the autocatalytic nature of the avalanche breakthrough at low temperatures. The natural frequency of this process is about 1 kHz. The experimental system can be explained by a phenomenological Rashevsky-Turing reaction-diffusion model [23], consistent with the fact that many degrees of freedom are potentially involved (but need not to be active).

For the dynamical behavior, again the presence of homoclinic tangency points should be reflected by a straight-line part on the l.h.s. in the scaling function $\phi(\lambda)$. This effect can be observed if other, competing mechanisms are absent [19]. Figure 4 is consistently interpreted in this way. This particular form of the scaling function derives from the fact that the original time series has been taken at conditions far away from crisis. Along with the dynamical phase-transition-like effect, a similar effect has been detected in the probabilistic scaling function $f(\alpha)$ (see Figure 5). The specific shape of the $f(\alpha)$ curve might be induced by the same mechanism as responsible for the behavior of the $\phi(\lambda)$ curve.

The ruby NMR laser [24] through its variety of nonlinear behavior is one of the ideal systems for an experimental application. Its behavior results from a strong nonlinear reaction to weak external modulation of parameters at low frequencies (~ 100 Hz). Upon alteration of the modulation amplitude (experimentally, in most cases the quality factor of the resonator cavity was modulated, but also other possibilities exist), the most prominent features which can be observed are bifurcations of different types and crises. The latter are triggered off by a collision between attractors and unstable trajectories. For low modulation amplitudes, the NMR laser can be described in a satisfactory way by Lorenz-type equations derived from the Bloch-Kirchhoff equations. Due to necessary adiabatic elimination, in order to achieve chaotic behavior, the phase space has to be enlarged by parametric modulation. Let us point out, however, that for higher modulation amplitudes the system shows fractal dimensions larger than three and more than one positive Lyapunov exponent. Using a term coined by Rössler [25], the latter states can be called "hyperchaotic". In this case, the former set of equations is no longer sufficient, and for a description of the system other transitions than the spin $1/2 \rightarrow -1/2$ transition have to be taken into account.

In the following, we present for two exemplary experimental files, taken at different small modulation

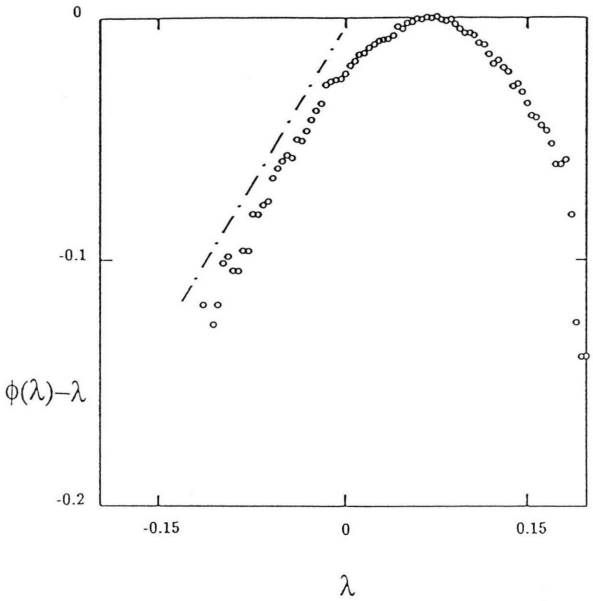

Fig. 6. Phase-transition-like effect in the dynamical scaling function $\phi(\lambda)$ for the experimental NMR laser, far away from a crisis, due to the presence of homoclinic tangency points.

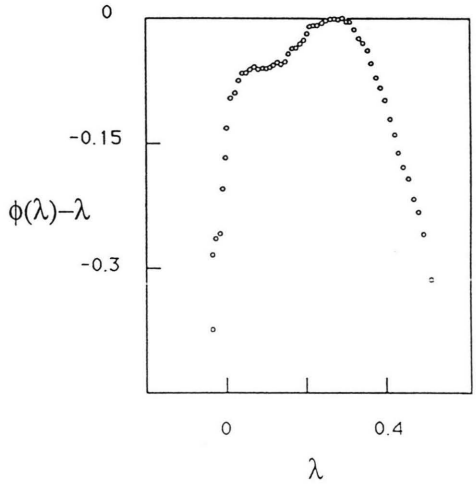

Fig. 7. Phase-transition-like effect in the dynamical scaling function $\phi(\lambda)$ for the experimental NMR laser due to the presence of a crisis.

amplitudes, the scaling functions of the Lyapunov exponents (see Fig. 6 and Figure 7). From data files of at least 250,000 integers recorded with 12 bit resolution, the Lyapunov exponents have been calculated, and the scaling functions have been derived. Each one of the files is characteristic for one of the two dynamical phase transitions mentioned above. The first one describes an experimental situation far from a crisis, whereas the second occurred just after a crisis. With reference to the theoretical outline given above, we focus now on two particularities of the scaling functions. In the first file (Fig. 6), we note the straight-line behavior on the left hand side of the scaling function which is due to the presence of homoclinic tangency points. In the second file (Fig. 7), a two-humped structure becomes evident. The first hump in the scaling function is to be interpreted as the remainder of a previously merged chaotic attractor after an attractor-merging crisis. The present situation should be compared with the results of [19]. There, an attractor-merging crisis was observed and discussed for the circle map model. The resulting scaling function turns out to be almost identical with the scaling function of the NMR laser after the crisis.

7. Conclusion

Theoretically predicted phase transitions could be detected from experimental germanium semiconductor and ruby NMR-laser files. In this way, it is indicated that scaling functions are a powerful means for the characterization of experimental data. For instance, visual observation of a crisis has been corroborated with the help of the calculated scaling function and by comparison with the behavior of a well-known model system. Following this way, one might be led to new insights into experimental systems (for an example, see [26]).

Acknowledgements

The authors would like to thank T. Tél for fruitful communications. They benefitted from experimental data provided by the Tübingen semiconductor group and the Zurich laser group.

[1] T. C. Halsey, M. H. Jensen, L. P. Kadanoff, I. Procaccia, and B. Shraiman, Phys. Rev. **A 33,** 1141 (1986).
[2] M. Kohmoto, Phys. Rev. **A 37,** 1345 (1988).
[3] a) Y. Oono and Y. Takahashi, Prog. Theor. Phys. **63,** 1804 (1980); b) J. P. Eckmann and I. Procaccia, Phys. Rev. **A 34,** 659 (1986); c) M. Sano, S. Sato, and Y. Sawada, Prog. Theor. Phys. **76,** 945 (1986); d) P. Szepfalusy and T. Tél, Phys. Rev. **A 34,** 2520 (1986); e) T. Horita, H. Hata, H. Mori, T. Morita, and K. Tomita, Prog. Theor. Phys. **80,** 923 (1988); f) R. Stoop, J. Peinke, J. Parisi, B. Röhricht, and R. P. Huebener, Physica **D 35,** 425 (1989).
[4] A. Renyi, Probability Theory, North-Holland, Amsterdam 1970.
[5] P. Grassberger and I. Procaccia, Physica **D 13,** 34 (1984).
[6] T. Bohr and D. Rand, Physica **D 25,** 387 (1987).
[7] R. Stoop, J. Parisi, and H. Brauchli, Z. Naturforsch. **64a,** 642 (1991).
[8] R. Stoop, Z. Naturforsch. **46a,** 1117 (1991).
[9] P. Szepfalusy, T. Tél, A. Csordas, and Z. Kovacs, Phys. Rev. **A 36,** 3525 (1987).
[10] M. J. Feigenbaum, I. Procaccia, and T. Tél, Phys. Rev. **A 39,** 5359 (1989).
[11] Z. Kaufmann and P. Szepfalusy, Phys. Rev. **A 40,** 2615 (1989).
[12] P. Cvitanovic, G. Gunaratne, and I. Procaccia, Phys. Rev. **A 38,** 1503 (1988).
[13] P. Grassberger and H. Kantz, Phys. Lett. **A 113,** 235 (1985).
[14] Ya. G. Sinai, Russ. Math. Surv. **27,** 21 (1972); R. Bowen, Lect. Not. Math. **470,** Springer, Berlin 1975; D. Ruelle, Thermodynamic Formalism, Addison-Wesley, Reading MA 1978.
[15] T. Tél, Z. Naturforsch. **43a,** 1154 (1988).
[16] S. Newhouse, Dynamical Systems, Birkhaeuser, Boston 1980.
[17] J. Guckenheimer and P. Holmes, Nonlinear Oscillations, Dynamical Systems, and Bifurcations of Vector Fields, Springer, New York 1986.
[18] C. Grebogi, E. Ott, and J. A. Yorke, Phys. Rev. Lett. **48,** 1507 (1982).
[19] T. Horita, H. Hata, H. Mori, T. Morita, S. Kuroki, and H. Okamoto, Prog. Theor. Phys. **80,** 809 (1988).
[20] R. Stoop and P. F. Meier, J. Opt. Soc. Amer. **B 5,** 1037 (1988).
[21] R. Stoop and J. Parisi, Physica **D 50,** 89 (1991).
[22] J. Peinke, J. Parisi, O. E. Rössler, and R. Stoop, Chaos in Experiment, Springer, Berlin (to be published 1992).
[23] J. Parisi, J. Peinke, B. Röhricht, U. Rau, M. Klein, and O. E. Rössler, Z. Naturforsch. **42a,** 655 (1987).
[24] P. Boesiger, E. Brun, and D. Meier, Phys. Rev. Lett. **38,** 602 (1977).
[25] O. E. Rössler, Phys. Lett. **71 A,** 155 (1979).
[26] J. Parisi, J. Peinke, R. P. Huebener, R. Stoop, and M. Duong-van, Z. Naturforsch. **44a,** 1046 (1989).